The Journal of Immunology
RESEARCH ARTICLE | JULY 01 2022

# Extracellular pH Controls Chemotaxis of Neutrophil Granulocytes by Regulating Leukotriene $B_4$ Production and Cdc42 Signaling

Leonie Oster; ... et. al

*J Immunol* (2022) 209 (1): 136–144.
https://doi.org/10.4049/jimmunol.2100475

# Extracellular pH Controls Chemotaxis of Neutrophil Granulocytes by Regulating Leukotriene $B_4$ Production and Cdc42 Signaling

**Leonie Oster,[1] Julia Schröder,[1] Micol Rugi, Sandra Schimmelpfennig, Sarah Sargin, Albrecht Schwab, and Karolina Najder**

**Neutrophil granulocytes are the first and robust responders to the chemotactic molecules released from an inflamed acidic tissue. The aim of this study was to elucidate the role of microenvironmental pH in neutrophil chemotaxis. To this end, we used neutrophils from male C57BL/6J mice and combined live cell imaging chemotaxis assays with measurements of the intracellular pH ($pH_i$) in varied extracellular pH ($pH_e$). Observational studies were complemented by biochemical analyses of leukotriene $B_4$ ($LTB_4$) production and activation of the Cdc42 Rho GTPase. Our data show that $pH_i$ of neutrophils dose-dependently adapts to a given pH of the extracellular milieu. Neutrophil chemotaxis toward C5a has an optimum at $pH_i$ ~7.1, and its $pH_i$ dependency is almost parallel to that of $LTB_4$ production. Consequently, a shallow $pH_e$ gradient, resembling that encountered by neutrophils during extravasation from a blood vessel (pH ~7.4) into the interstitium (pH ~7.2), favors chemotaxis of stimulated neutrophils. Lowering $pH_e$ below pH 6.8, predominantly affects neutrophil chemotaxis, although the velocity is largely maintained. Inhibition of the $Na^+/H^+$ exchanger 1 (NHE1) with cariporide drastically attenuates neutrophil chemotaxis at the optimal $pH_i$ irrespective of the high $LTB_4$ production. Neutrophil migration and chemotaxis are almost completely abrogated by inhibiting $LTB_4$ production or blocking its receptor (BLT1). The abundance of the active GTP-bound form of Cdc42 is strongly reduced by NHE1 inhibition or $pH_e$ 6.5. In conclusion, we propose that the pH dependence of neutrophil chemotaxis toward C5a is caused by a $pH_i$-dependent production of $LTB_4$ and activation of Cdc42. Moreover, it requires the activity of NHE1.** ***The Journal of Immunology*****, 2022, 209: 136–144.**

Neutrophil granulocytes are the first immune cells to arrive at a site of inflammation. Guided by chemoattractants, they extravasate and migrate toward affected sites to deploy their defense mechanisms (1). Robust neutrophil effector functions help to fight against invading pathogens, but an inadequate neutrophil response can also be harmful for the host. In severe inflammation, dysfunctional neutrophils can impede the activity of other cells of innate and adaptive immunity (2). Recently, neutrophil dysfunction was shown to contribute to thrombotic events in COVID-19 patients (3).

The inflammatory microenvironment often acidifies because of lactate release, tissue oxygen deprivation, and primarily glycolytic metabolism of the arriving neutrophils (4). Production of reactive oxygen and nitrogen species during the respiratory burst of neutrophils leads to an $H^+$ efflux mediated by $H^+$ channels and in part by $Na^+/H^+$ exchanger 1 (NHE1). Thus, increased neutrophil activity adds to the acidification of the inflammatory microenvironment (5–7), which in turn will also affect the intracellular pH of neutrophils.

It is known that low extracellular pH ($pH_e$) elicits either proinflammatory or anti-inflammatory effects. For instance, NETosis, one of the major defense mechanisms of neutrophils, is inhibited by the acidity (8). An acidic environment also prolongs the survival of neutrophils (4). The remarkable ability of neutrophils to survive in an acidic oxygen- and glucose-deprived environment, which is characteristic for autoimmune diseases, chronic inflammation, and solid tumors, often leads to unfavorable neutrophil dysfunction and retention. Neutrophil activity thereby often contributes to the burden of the above-mentioned conditions (9, 10). The acidic pH of the inflammatory microenvironment may influence neutrophil chemotaxis in a dual way: rendering neutrophils unable to reach the site of inflammation or, on the contrary, causing excessive neutrophil accumulation. Therefore, it is important to understand the pH-dependent regulation of the mechanisms underlying chemotaxis to open opportunities to new therapeutic targets or optimize existing ones.

Neutrophil chemotaxis is initiated by end-target chemoattractants such as complement molecule C5a and formylated peptides, which are secreted at the site of inflammation and employ mainly the p38/MAPK pathway in neutrophils. Once activated, the neutrophils themselves release intermediary chemoattractants such as leukotriene $B_4$ ($LTB_4$) or IL-8, which bind to the $LTB_4$ receptor (BLT1) or IL-8R and act via the PI3K/Akt pathway, boosting the immune response in autocrine and paracrine ways (11, 12). There is a close interrelationship between end-target and intermediary chemoattractants, which can be exemplified by the C5a/$LTB_4$/BLT1 axis. C5a-stimulated neutrophils

Institute of Physiology II, Westfälische Wilhelms University, Münster, Germany

[1]L.O. and J.S. contributed equally to this work.

ORCIDs: 0000-0002-4291-0374 (L.O.), 0000-0002-0649-0923 (K.N.).

Received for publication May 20, 2021. Accepted for publication April 27, 2022.

This work was supported by Deutsche Forschungsgemeinschaft Grants SCHW 407/17-1 and GRK 2515/1, Chembion; the 2020 Marie Skłodowska-Curie Actions Innovative Training Network (Grant 813834-pHioniC-H2020-MSCA-ITN-2018); and by Interdisziplinäres Zentrum für Klinische Forschung Münster Grant Schw2/020/18.

Address correspondence and reprint requests to Albrecht Schwab, Institut für Physiologie II, Robert-Koch-Strasse 27b, 48149 Münster, Germany. E-mail address: aschwab@uni-muenster.de

The online version of this article contains supplemental material.

Abbreviations used in this article: BCECF 2′, 7′-bis(carboxyethyl)-5(6)-carboxyfluorescein; CI, chemotaxis index; 3D, three-dimensional; $LTB_4$, leukotriene $B_4$; NHE1, $Na^+/H^+$ exchanger 1; $pH_e$, extracellular pH; $pH_i$, intracellular pH; PI, propidium iodide.

release $LTB_4$ and thereby reinforce chemotaxis and cause neutrophil swarming toward the inflamed site or injured tissue. This "relay" mechanism is essential for proper neutrophil chemotaxis (13, 14).

The way in which pH affects neutrophil chemotaxis could manifest itself in a disruption of the C5a/$LTB_4$/BLT1 axis and consequently altered activation of downstream effectors such as Cdc42. This would lead to a pH dependence of chemotaxis because Cdc42 regulates neutrophil polarization, actin polymerization, and C5a receptor internalization (15–18). In dendritic cells, inhibition of BLT1 signaling disrupts Cdc42 activation and actin polymerization (19). However, BLT1–Cdc42 interaction and its pH dependence have not yet been investigated in neutrophils. Because neutrophil migration in a three-dimensional (3D) environment relies on actin rearrangements (20), it is possible that a pH-dependent modulation of Cdc42 activity will also affect neutrophil motility.

We show in our studies that chemotaxis of C5a-stimulated neutrophils in a 3D collagen matrix is indeed strongly pH- and NHE1-dependent. Our results suggest that the inhibition of neutrophil chemotaxis toward C5a by extracellular acidity can be explained by a pH-dependently reduced $LTB_4$ secretion and impaired Cdc42 signaling. Thus, the extracellular acidity or NHE1 inhibition causes an intracellular acidification that in turn is responsible for the observed inhibition of chemotaxis.

## Materials and Methods

All chemicals were purchased from Sigma-Aldrich (Steinheim am Albuch, Germany) unless stated otherwise.

### *Mice*

Wild-type C57BL/6J male mice (Charles River Laboratories) were used for all experiments, and at least $N = 3$ mice were used for each condition. Animals were euthanized by cervical dislocation. Experimental protocols were approved by the local Committee for Animal Care with permit number 84-02.05.50.15.010.

### *WEHI-3B conditioned medium*

Myelomonocytic leukemia cells (WEHI-3B) were cultivated at 37°C and 5% $CO_2$ in DMEM medium containing 10% FCS (heat inactivated), 2 mM L-glutamine, and 1% penicillin/streptomycin. The cells were cultured for 5 d. Conditioned medium was then collected, sterile filtered, and stored at −20°C for later use.

### *Isolation of neutrophils*

Neutrophils were isolated from murine bone marrow as described earlier (21). In brief, the tibia and femur were flushed with HBSS without $Ca^{2+}$ and $Mg^{2+}$ ions ($HBSS^{-/-}$, Merck Chemicals, Darmstadt, Germany) containing 10% FCS (Life Technologies/Thermo Fisher Scientific, Dreieich, Germany) and 25 mM HEPES (pH 7.2). The resulting suspension was filtered through a 70-μm nylon mesh and centrifuged at 200 × *g* for 10 min. The cell pellet was resuspended in 1 ml of $HBSS^{-/-}$ with 25 mM HEPES, gently layered on top of a density gradient (1.077 and 1.119 g/ml Pancoll, PAN-Biotech, Aidenbach, Germany) and centrifuged at 677 × *g* for 30 min. Collected neutrophils were washed twice with $HBSS^{-/-}$ containing 10% FCS and 25 mM HEPES and centrifuged at 200 × *g* for 10 min. The neutrophils were then resuspended in RPMI 1640 medium containing 1% penicillin/streptomycin, 5% heat-inactivated FCS, and 5% WEHI-3B conditioned medium. Cells were cultured overnight at 37°C, 5% $CO_2$ in a Ø10-cm petri dish. The purity of neutrophil preparations was analyzed by immunocytochemistry using an FITC anti-mouse Ly-6G Ab (clone 1A8, BioLegend, San Diego, CA). Ly-$6G^+$ cells comprised ~85% of nucleated cells.

### *Flow cytometry analysis of cell viability*

A propidium iodide (PI) flow cytometric assay was performed to determine the viability of the cells. Neutrophils were centrifuged and resuspended in Ringer's solution (140 mM NaCl, 5.4 mM KCl, 1.2 mM $CaCl_2$, 0.8 mM $MgCl_2$, 10 mM HEPES, 5.5 mM glucose; adjusted to $pH_e$ 6.5 or $pH_e$ 7.4) after overnight incubation. Then neutrophils were stimulated with 60 nM C5a with or without 10 μM zileuton and incubated for 1 h at 37°C. After centrifugation, cells were resuspended in 10 μg/ml PI in PBS with 1 mM $Ca^{2+}$ and 1 mM $Mg^{2+}$ ions, containing 0.1% albumin. Cells were analyzed using a Guava easyCyte 5 flow cytometer (Merck Millipore, Darmstadt, Germany). Following doublet discrimination, cells were gated for $PI^+$ cells based on unstained control samples.

### *3D chemotaxis assay in varied extracellular pH*

Chemotaxis was monitored in μ-slides for chemotaxis (catalog no. 80326, Ibidi, Gräfelfing, Germany). Neutrophils were used after 16 h of overnight differentiation. The surface of the chemotaxis channel was coated with 25 μg/ml fibronectin (Roche Diagnostics, Penzberg, Germany) for 1 h. Neutrophils were suspended in HEPES-buffered Ringer's solution (pH 7.4). Then, cells were mixed with collagen I (rat tail, final concentration 2.5 mg/ml, Corning Life Sciences, Corning, NY) in HBSS containing 1 mM $Ca^{2+}$ and 1 mM $Mg^{2+}$ ($HBSS^{+/+}$) buffered with HEPES (25 mM) and adjusted to the desired pH value. When needed this mixture was supplemented with the respective inhibitors (the final concentrations are given in parentheses): NHE1 inhibitor cariporide (10 μM), 5-lipoxygenase inhibitor zileuton (10 μM), BLT1 blocker LY223982 (10 μM; Cayman Chemical, Ann Arbor, MI).

The chemotaxis channel was filled with the collagen mixture containing $2 \times 10^5$ neutrophils and incubated at room temperature for 10 min. Afterwards, the chambers were filled with HEPES-buffered Ringer's solution of the desired pH value, and the chemoattractant (C5a; 60 nM, R&D Systems, Wiesbaden, Germany) was added to one of the chambers to create a chemotactic gradient. The optimal C5a concentration (60 nM) for chemotaxis was established by comparing concentrations of 6, 60, and 370 nM C5a (see Supplemental Fig. 1).

Migrating cells were observed under a phase contrast microscope (Axiovert 40; Zeiss, Jena, Germany) connected to a camera (XC-77CE; Hamamatsu [Hamamatsu, Japan] or Bresser MikroCam SP 3.1 [Bresser, Rhede, Germany]). Images were acquired in 5-s intervals for 30 min. The recording started 20 min after establishing the chemoattractant gradient. Pilot experiments had shown that the chemotaxis index of neutrophils is stable after that time. The movement was tracked with Amira software (Thermo Fisher Scientific, Waltham, MA). Segmented image stacks were processed using ImageJ software (https://imagej.nih.gov/ij/) and a self-made plugin (22). Chemotaxis was quantified with the following parameters: velocity calculated as a three-point difference quotient; total distance covered during the course of the experiment and net movement parallel to the direction of the chemotactic gradient. The chemotactic index (CI) is calculated for each cell by dividing the net movement into the direction of the chemotactic gradient by the total distance.

### *3D chemotaxis in a pH gradient*

For monitoring 3D chemotaxis in a pH gradient (pH-taxis), the chambers were filled with HEPES-buffered Ringer's solutions adjusted to pH 8.0 and 4.5, respectively. This results in a pH gradient within the collagen matrix ranging from pH 7.45 to 7.2 as quantitatively assessed using 2′,7′-bis(carboxyethyl)-5(6)-carboxyfluorescein (BCECF) acid as an extracellular pH indicator. To this end, the 3D collagen matrix containing 5 μg/ml BCECF was loaded into μ-slides for chemotaxis, and fluorescence emission intensities at 535 nm upon excitation at 480 and 440 nm were measured across the chemotaxis channel. These measurements were calibrated separately using identical μ-slides for chemotaxis filled with BCECF-containing collagen matrix adjusted either to pH 6.5 or 7.4, respectively. Absolute values of the established pH gradient were calculated from a linear regression based on the ratio of intensities (excitation 480/440 nm) in matrices of known pH. Image acquisition and data analysis were performed in the same way as described above (see *3D chemotaxis assay in varied extracellular pH*).

### *Determination of the $LTB_4$ concentration*

We determined the concentration of leukotriene $B_4$ ($LTB_4$) in the supernatant of neutrophils ($10^6$/0.5 ml) kept in HEPES-buffered Ringer's solution of different pH values (pH 6.5–7.4) using an $LTB_4$ Parameter ELISA assay kit (R&D Systems). The cells were stimulated with 60 nM C5a and incubated for 1 h at 37°C. The supernatant was collected after centrifugation and further processed according to the manufacturer's instructions. The kit provides a standard solution that allows calibration. We performed two technical duplicates for each measurement. The absorbance of the resulting reaction solution was measured at 500 nm in a THERMOmax microplate reader (Molecular Devices, San Jose, CA). The inhibitory efficacy of zileuton was determined by incubating C5a-stimulated cells with 0.1, 0.3, 1, 10, and 30 μM zileuton. Maximal inhibition of $LTB_4$ production was reached at a zileuton concentration of 10 μM (see Supplemental Fig. 2).

### *Determination of intracellular pH*

Intracellular pH ($pH_i$) was measured using the acetoxymethyl ester of BCECF (BCECF-AM) (Thermo Fisher Scientific, Waltham, MA). The acetoxymethyl form of the pH indicator can freely diffuse into the cytosol where it becomes charged upon hydrolysis and consequently trapped inside the cell. Neutrophils were seeded on fibronectin-coated (25 μg/ml) Ibidi slides I (catalog no. 80106) and loaded with BCECF-AM (2.5 μg/ml) for 3 min at 37°C. Then, slides were washed with HEPES-buffered Ringer's solution and put under the superfusion system mounted to the fluorescence microscope.

Image acquisition was controlled by VisiView software (Visitron Systems, Puchheim, Germany). Fluorescence emission intensities of the separate cells in the field of view were measured at 535 nm with excitation at 480 and 440 nm. Each measurement was followed by superfusion with $K^+$-rich calibration solutions (125 mM KCl, 1 mM $CaCl_2$, 1 mM $MgCl_2$, 20 mM HEPES; adjusted to pH 6.5, 7.0, 7.5, 7.8) containing 10 μM nigericin. After background subtraction, absolute pH values were calculated ratiometrically (480/440 nm) and based on linear regression of intensity ratios of calibration solutions. Separate analysis and calibration were done for each cell.

### *$NH_4^+$ prepulse method for assessing NHE1 activity*

The activity of NHE1 was determined using the previously described $NH_4^+$ prepulse (or acid loading) method (23, 24). Shortly, cells were superfused with a solution containing $NH_4Cl$ (102.5 mM NMDG-HCl, 20 mM $NH_4Cl$, 5.4 mM KCl, 1.2 mM $CaCl_2$, 0.8 mM $MgCl_2$, 1 mM $BaCl_2$, 10 mM HEPES, 5.5 mM glucose), which dissociates to cell-permeable $NH_3$. After entering the cell, $NH_3$ binds to protons causing an intracellular alkalinization. Subsequent exchange to a $Na^+$- and $NH_4^+$-free solution (122.5 mM NMDG-HCl, 5.4 mM KCl, 1.2 mM $CaCl_2$, 0.8 mM $MgCl_2$, 10 mM HEPES, 5.5 mM glucose) causes the dissociation of $NH_4^+$ and $NH_3$ diffusion out of the cell. Rapid accumulation of $H^+$ occurs due to inhibition of the NHE1 in the absence of $Na^+$. The speed of $pH_i$ recovery (ΔpH/min) upon readdition of extracellular $Na^+$ is a measure of NHE1 activity. The contribution of NHE1 to pH recovery was further assessed by supplementing the $Na^+$ containing HEPES Ringer's solution with 10 μM cariporide.

### *Cdc42-GTP pull-down and Western blotting*

Cdc42 activity in neutrophils was quantified using a Cdc42 activation assay biochem kit (Cytoskeleton, Denver, CO). The total Cdc42 was compared with the active, GTP-bound form. Prior to C5a stimulation, neutrophils were equilibrated at 37°C in Ringer's solution of the desired $pH_e$ value for 10 min. Neutrophils were stimulated with 60 nM C5a in Ringer's solution at pH 6.5 and 7.4 for 1 min. Alternatively, neutrophils were stimulated with 60 nM C5a in Ringer's solution at $pH_e$ 6.5 and 7.4 for 20 min. When performing experiments with NHE1 inhibition, neutrophils were either stimulated with 60 nM C5a in presence of 10 μM cariporide at 37°C for 1 min or first incubated with 10 μM cariporide at 37°C for 10 min and then stimulated with 60 nM C5a for 1 min. Cells were lysed in lysis buffer containing protease inhibitors provided by the manufacturer. To achieve the required protein concentration, lysates of neutrophils from two to three mice were pooled for each experiment. Equal loading was ensured by measuring the protein concentration of the samples with a Pierce BCA protein assay kit (Thermo Fisher Scientific, Waltham, MA). The individual steps of the pull-down assay were performed according to the manufacturer's instructions with some modifications. Following pull-down, total protein and corresponding precipitates were loaded onto a 10% polyacrylamide gel. GTPγS-treated lysates served as positive controls. The membrane was incubated overnight with a 1:250 dilution of anti-Cdc42 primary Ab (mouse, clone 4B3) at 4°C. The membrane was further incubated with goat-anti-mouse HRP Ab (1:25,000) for 1 h at room temperature. The signal was detected using Super-Signal west femto (Thermo Fisher Scientific, Waltham, MA), and chemiluminescence intensities were compared using Image Lab software version 6.1 (Bio-Rad Laboratories, Hercules, CA). Background-subtracted intensities resulting from precipitated Cdc42 protein were set in relationship to that of total Cdc42 protein.

### *Statistical analysis*

All values are given as mean ± SEM unless indicated otherwise. For comparison between two groups, an unpaired Student *t* test was used for normally distributed data, or a Mann–Whitney test was used for non-normally distributed data. More than two groups were compared with a one-way ANOVA with a Tukey post hoc or Kruskal–Wallis test with a Dunn's post hoc test. An "*N*" indicates the number of mice used in the experiments, whereas "*n*" indicates the number of single cells analyzed. A $p$ value $<0.05$ was considered statistically significant. Analyses were performed with GraphPad Prism version 8.3.1 for Windows (GraphPad Software, San Diego, CA; https://www.graphpad.com) and R programming language (version 4.0.3; https://www.R-project.org/).

## Results

### *Neutrophil chemotaxis in a C5a gradient is pH-dependent and requires NHE1 activity*

The ability of neutrophils to navigate toward an inflamed site is affected by the changing environment. In our studies, we analyzed neutrophil chemotaxis and NHE1 activity in a pH range from $pH_e$ 6.5 to 7.4. Pilot experiments had shown that chemotaxis is optimal with 60 nM C5a (Supplemental Fig. 1). Neutrophil chemotaxis toward C5a is clearly dependent on the ambient pH value and on NHE1 activity. Fig. 1A shows the trajectories of individual neutrophils migrating in 3D collagen I gels and monitored for 30 min. Tracks are normalized to common starting points on the *y*-axis, which is in parallel to the chemotactic C5a gradient (gray bar). Neutrophils were exposed to $pH_e$ 6.5, 6.8, 7.0, and 7.4. The lower panel illustrates trajectories of neutrophils upon NHE1 inhibition, and Fig. 1B and 1C provide the summary of neutrophil

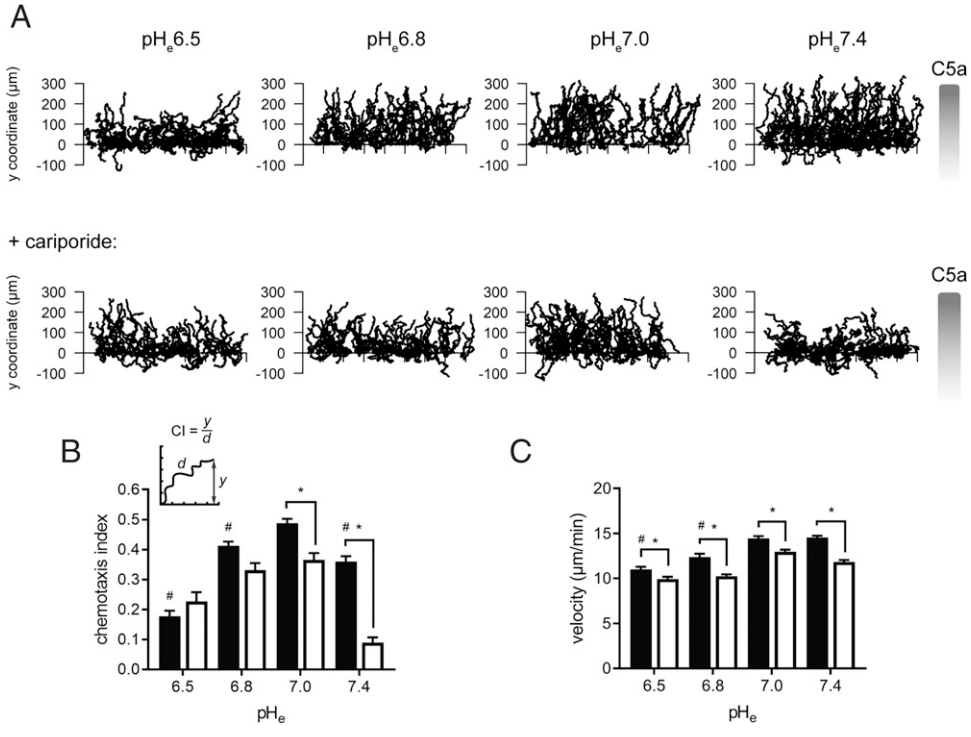


**FIGURE 1.** Extracellular pH and NHE1 activity predominantly regulate neutrophil chemotaxis toward C5a. (**A**) Trajectories of individual neutrophils migrating in a 3D collagen I matrix. They are exposed to a C5a gradient in $pH_e$ 6.5, 6.8, 7.0, and 7.4. The direction of the C5a gradient is indicated on the right-hand side. The lower panels show the trajectories of neutrophils in the presence of the NHE1 inhibitor cariporide. All trajectories are normalized to common starting points along the *y*-axis, which represents the direction of the C5a gradient. (**B**) Chemotaxis indices and (**C**) velocity of neutrophils migrating in different $pH_e$ environments without (closed bars) and with NHE1 inhibition (open bars) ($N \geq 3$, $n \geq 60$, Kruskal–Wallis, Dunn's post hoc, $^*p < 0.05$, $^{\#}p < 0.05$ versus optimum at $pH_e$ 7.0).

chemotaxis and velocity, respectively. It becomes clearly evident that the CI in a range from $pH_e$ 6.5 to 7.4 has a bell-shaped pH dependence with an optimum at $pH_e$ 7.0. Importantly, neutrophil viability does not decrease in $pH_e$ as low as pH 6.5 as quantified by flow cytometry (see Supplemental Fig. 3). NHE1 inhibition leads to a massive decrease of neutrophil chemotaxis at $pH_e$ 7.0 and 7.4 (at $pH_e$ 7.4 by ~75%). At lower $pH_e$, NHE1 inhibition evokes almost no further inhibition of the already impaired chemotaxis.

Neutrophil velocity is also affected by the extracellular pH. However, relative changes of this parameter are not as pronounced as those of the chemotaxis index. An extracellular acidification to $pH_e$ 6.5 induces a reduction of the velocity by ~25%. In contrast to neutrophil directionality, the ability of neutrophils to roam the acidic environment, although diminished, is largely preserved. The simultaneous inhibition of the NHE1 leads to a further decrease of the velocity by an additional 10–20% for each of the tested $pH_e$ values. Taken together, these results indicate that neutrophil chemotaxis (directionality) rather than the migration motor (velocity) is particularly dependent on the "correct" ambient $H^+$ concentration and NHE1 activity.

### *A $pH_e$ gradient induces moderate directional migration of neutrophils and strengthens the effect of a C5a gradient*

In the next set of experiments, we studied the impact of a $pH_e$ gradient per se (from $pH_e$ 7.2 to 7.45) and its combination with a C5a gradient (60 nM C5a) on neutrophil chemotaxis. This allowed us to mimic in vivo conditions in which inflammation is a source of both protons and chemoattractants. When investigating the effect of a proton gradient per se, we analyzed the movement of neutrophils from three horizontal sections (I, II, and III) of the visual field separately (Fig. 2A). However, when studying the combined effect of a proton and a C5a gradient, we had to divide the field of view into two horizontal sections (I and II, Fig. 2B) because C5a-stimulated neutrophils cover longer net distances during the course of the experiment. By analyzing neutrophils residing in spatially distinct sections separately, we could link neutrophil chemotaxis to a range of $pH_e$ values within the $pH_e$ gradient. When no $pH_e$ gradient was imposed (upper panel in Fig. 2C), all neutrophils were exposed to $pH_e$ 7.4.

The $pH_e$ gradient alone induces moderate neutrophil directionality in sections II and III (CI ~0.05; $p < 0.05$). In the most acidic section (I, $pH_e$ ~7.2) neutrophils migrate in a random fashion (CI ~0) (Fig. 2A). As expected, addition of C5a induces efficient chemotaxis (Fig. 2B). When applying the same analysis algorithm for the two sections I and II, the mean chemotaxis index does not differ. However, analysis of chemotaxis *over time* reveals that the chemotaxis index of C5a-stimulated neutrophils steadily increases in the more acidic section (Fig. 2C, lower graph). This is not the case for those cells that reside in the more alkaline half of the $pH_e$ gradient. Thus, the combination of a chemoattractant (C5a) and shallow $H^+$ gradient amplifies the chemotactic response. Such a behavior is not observed in the absence of a $pH_e$ gradient (Fig. 2C, upper graph). Regardless of the spatial position within the visual field, chemotaxis toward C5a alone (i.e., in the absence of an additional pH gradient) reaches an optimum after ~20 min and declines thereafter. Collectively, our results show that a $pH_e$ gradient approaching $pH_e$ 7.2 favors neutrophil chemotaxis. Thus, as opposed to *Amoeba proteus* (25), an extracellular proton gradient is rather a modulator of neutrophil chemotaxis than a strong chemoattractant itself.

### *NHE1 determines $pH_i$ dynamics of stimulated neutrophils*

Neutrophils arriving at the site of inflammation are influenced by both acidic pH and abundant chemoattractants. To assess the impact of the acidic environment on neutrophil $pH_i$, we first measured $pH_i$ while superfusing the cells with HEPES-buffered Ringer's solution adjusted to $pH_e$ 6.5 (Fig. 3A). The change from the physiological $pH_e$ 7.4 to the acidic $pH_e$ 6.5 leads to a slow decrease of the cytoplasmic $pH_i$ of neutrophils that reaches a plateau at $pH_i$ 6.90 ± 0.04 within 5 min.

Next, we examined the combined effect of an extracellular acidification and the stimulation with C5a on $pH_i$. To dissect the changes of neutrophil $pH_i$ in varied $pH_e$ upon C5a stimulation, we preincubated the cells in HEPES-buffered Ringer's solution at $pH_e$ 6.5, 7.0, and 7.4 for ~10 min and then added C5a (Fig. 3B). To assess the role of NHE1 in neutrophil stimulation in solutions of different $pH_e$, we additionally conducted these measurements in the presence of 10 μM cariporide.

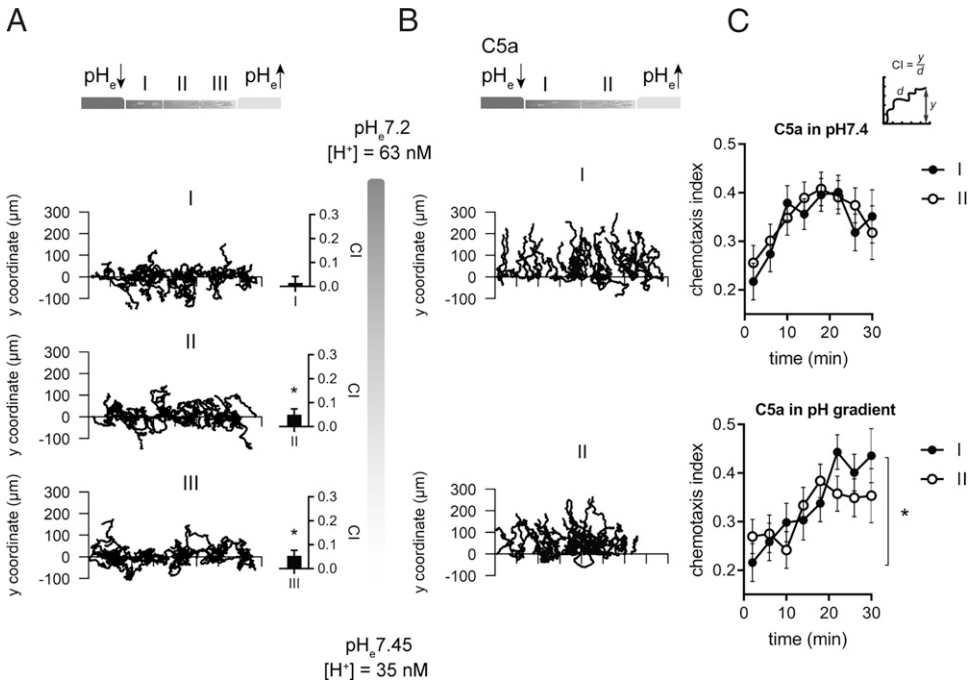


**FIGURE 2.** Neutrophil pH-taxis. (**A**) Trajectories and pH-taxis indices (left) of neutrophils migrating in a $pH_e$ gradient. The position of the sections I, II, and III in the pH gradient are indicated in the pictogram above the trajectories (*$p < 0.05$, compared with 0). (**B**) Trajectories of C5a-stimulated neutrophils in a $pH_e$ gradient. The positions of sections I and II in the pH gradient are indicated in the pictogram above the trajectories. (**C**) Comparison of chemotaxis indices of C5a-stimulated neutrophils in sections I and II over time. The upper graph shows chemotaxis over time when there is no pH gradient. The lower graph depicts chemotaxis toward C5a in a $pH_e$ gradient. Closed and open circles indicate sections closer and farther away from the chemoattractant source (control, $N \geq 3$, $n \geq 60$; pH gradient, $N \geq 4$, $n \geq 40$).

As shown in Fig. 3A, the $pH_i$ of neutrophils depends on the extracellular pH. When kept in acidic $pH_e$, the $pH_i$ follows, but does not exactly reach the value of the extracellular pH. This is illustrated by the distinct starting points of each curve in Fig. 3B. Stimulation with C5a (solid lines) causes a drop of $pH_i$. At $pH_e$ 6.5 the $pH_i$ decrease develops more slowly. Additional inhibition of NHE1 (dashed lines) strongly amplifies the C5a-induced acidification of the $pH_i$ in neutrophils. Thus, $pH_i$ of C5a-stimulated neutrophils not only depends on the ambient $pH_e$, but it is also importantly regulated by NHE1.

We finally demonstrated NHE1 activity in neutrophil $pH_i$ regulation by means of the ammonium prepulse technique. Following an intracellular acidification, $pH_i$ rapidly recovers in a $Na^+$-dependent and cariporide inhibitable way (Fig. 4A). The differences of the rate of $pH_i$ changes within 1 min of $Na^+$ readdition relate to the NHE1 involvement in $pH_i$ recovery (Fig. 4B).

*$LTB_4$ release depends on $pH_e$*

$LTB_4$ plays a major role in neutrophil chemotaxis in a C5a gradient (14, 26). We therefore tested whether the secretion of $LTB_4$ is pH-dependent. To this end we quantified $LTB_4$ in the supernatant of neutrophils stimulated with 60 nM C5a using an ELISA assay. To validate the assay and confirm increased $LTB_4$ production upon stimulation, we performed control experiments (at $pH_e$ 7.41 ± 0.07) without and with C5a. Unstimulated neutrophils produce negligible amounts of $LTB_4$ (below the sensitivity of the assay), whereas C5a stimulation leads to a substantial increase of the $LTB_4$ concentration in the supernatant. Addition of zileuton (5-LOX inhibitor; 0.1, 0.3, 1, 10, and 30 μM) to stimulated neutrophils abrogates this response dose-dependently (see Supplemental Fig. 2).

Next, we determined in detail the pH dependence of the $LTB_4$ secretion of C5a-stimulated neutrophils. Fig. 5A illustrates that the secretion rate is highest at $pH_e$ 7.11 ± 0.06 and only declines slightly upon acidification to $pH_e$ 6.91 ± 0.05 (−8.9%). However, $LTB_4$ secretion drops sharply when $pH_e$ is further lowered to $pH_e$ 6.67 ± 0.05 or increased to $pH_e$ 7.41 ± 0.07. Addition of the NHE1 inhibitor cariporide modifies the $pH_e$ dependency of $LTB_4$ production. Surprisingly, cariporide enhances $LTB_4$ secretion at $pH_e$ 7.4 (Fig. 5B, 5C).

In Fig. 6, pH-dependent $LTB_4$ release and chemotaxis are plotted as a function of the respective extracellular pH. It is evident that the $LTB_4$ secretion has a similar $pH_e$ dependence as the chemotaxis under control conditions with the optimum at $pH_e$ 7.1 (Fig. 6A). However, addition of cariporide disrupts this parallel behavior leading to the highest $LTB_4$ production at $pH_e$ 7.4, while neutrophil chemotaxis is severely inhibited (Fig. 6B, 6C).

Importantly, as shown in Fig. 3, $pH_e$ affects $pH_i$ and in this manner may alter the intracellular processes. Therefore, we analyzed the $LTB_4$ production and chemotaxis as a function of $pH_i$. The same relationship as with $pH_e$ becomes apparent when $LTB_4$ production is compared with the intracellular $pH_i$ (Fig. 7A). The increase of the $LTB_4$ production in the presence of cariporide at $pH_e$ 7.4 can be explained by the fact that the resulting intracellular pH of $pH_i$ 7.1 corresponds to the optimal $pH_i$ for $LTB_4$ production under control conditions. Thus, NHE1 inhibition shifts the maximum $LTB_4$ secretion to more alkaline $pH_e$ values (Fig. 7A). Nonetheless, chemotaxis is almost completely inhibited in the presence of cariporide at $pH_i$ 7.1 (Fig. 7B, 7C). These observations strongly support an apparently obligatory role of NHE1 for chemotaxis. Its inhibition is able to override increased $LTB_4$ release. As shown below, cariporide impairs chemotaxis almost as efficiently as interfering with the $LTB_4$/BLT1 axis directly.

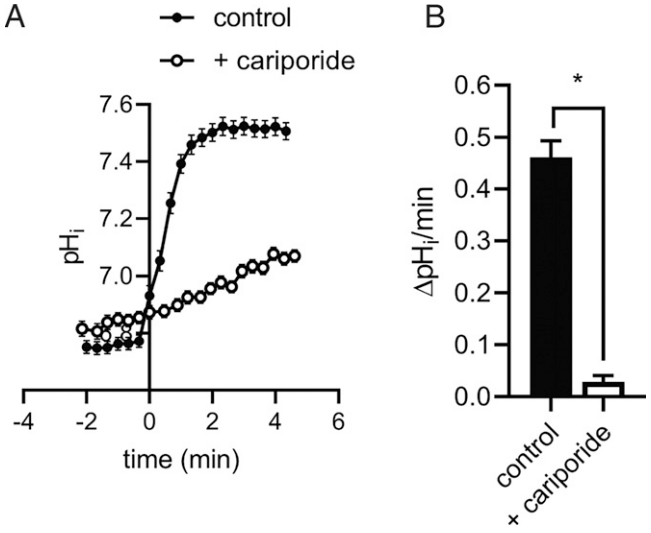


**FIGURE 4.** Neutrophil pHi recovery after acidification (ammonium prepulse) without or with NHE1 inhibition. (**A**) $pH_i$ of neutrophils superfused with $Na^+$-containing HEPES-buffered Ringer's solution (control, filled circles) and upon inhibition of NHE1 with cariporide (10 μM; open circles). (**B**) Summary of the $pH_i$ recovery rates within 1 min under control conditions and in the presence of the NHE1 inhibitor cariporide ($N \geq 4$, $n \geq 76$-111). *$p < 0.05$.

*Neutrophil chemotaxis is suppressed by interfering with the $LTB_4$/BLT1 axis*

The superimposition of chemotaxis indices and $LTB_4$ secretion (Fig. 6) suggests that the reduced $LTB_4$ secretion may be causally linked to the pH-dependent impairment of the chemotaxis. Therefore, we investigated the chemotactic behavior in a C5a gradient upon direct inhibition of the $LTB_4$/BLT1 axis. We inhibited either the production of $LTB_4$ using the 5-LOX inhibitor zileuton (10 μM) or blocked the $LTB_4$ receptor B1 (BLT1) with LY223982 (10 μM). As shown earlier (27), blocking the $LTB_4$ production or its receptor (almost) completely inhibits neutrophil chemotaxis. Fig. 8A shows the respective trajectories of neutrophils recorded at $pH_e$ 7.0. The summary of these experiments is

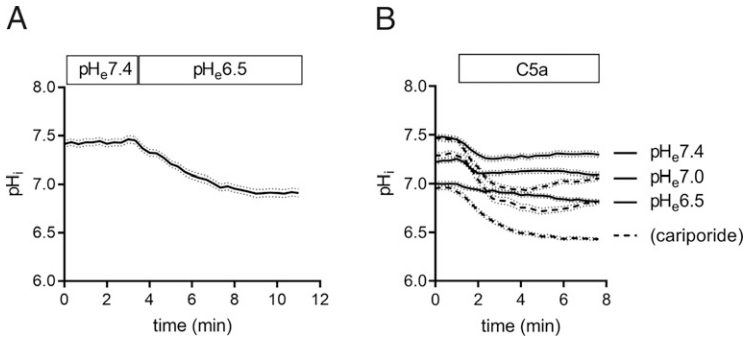


**FIGURE 3.** Influence of the acidic pHe, C5a stimulation, and NHE1 activity on neutrophil pHi. (**A**) $pH_i$ of neutrophils superfused with HEPES-buffered Ringer's solution of $pH_e$ 6.5. Neutrophil $pH_i$ reaches steady values of $pH_i$ 6.90 ± 0.04 after ~5 min. (**B**) Solid curves represent $pH_i$ changes of neutrophils kept in a range of distinct $pH_e$ values and stimulated with C5a. Dashed lines depict experiments with addition of the NHE1 inhibitor cariporide ($N \geq 3$, $n \geq 40$–102).

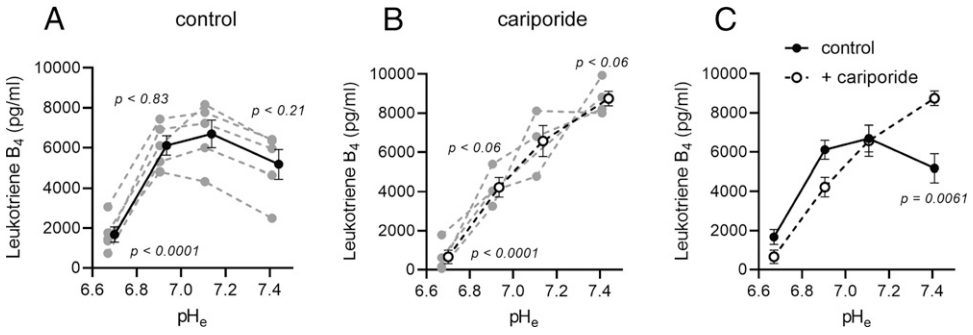


**FIGURE 5.** LTB4 secretion depends on pHe and NHE1 activity. Each dotted line connects measurements with neutrophils from the same mouse. The mean values for each condition are indicated in black. (**A**) The $LTB_4$ concentration in supernatants of neutrophils stimulated with 60 nM C5a in $pH_e$ ranging from $pH_e$ 6.67 to 7.41 ($N = 5$). (**B**) $LTB_4$ concentration of stimulated neutrophils upon NHE1 inhibition ($N \geq 3$) ($p$ values were determined using ANOVA with a Dunnett's post hoc test versus values at $pH_e$ 7.11). (**C**) Comparison between control and cariporide-treated neutrophils. The $p$ value indicates significant difference at $pH_e$ 7.4.

depicted in Fig. 8B and 8C. Both drugs, which are equally effective, strongly reduce the chemotaxis index and the migration velocity. It is conspicuous that the chemotaxis index declines even more than the velocity. However, the strong interference with the $LTB_4$/BLT1 axis overrides the $pH_e$ dependence so that any residual $pH_e$ dependence of neutrophil chemotaxis and migration cannot be interpreted with certainty.

*Cdc42 activation is inhibited by cariporide and an acidic $pH_e$*

Cdc42 is a member of Rho GTPases involved in neutrophil motility. The active Cdc42-GTP form is required for actin rearrangements at the leading edge of neutrophils, neutrophil polarization, and consequently proper chemotaxis (18). This is particularly relevant for neutrophils migrating in a 3D environment, which prioritizes the actin-based motility over the integrin-based motility on a two-dimensional surface (20). The former becomes essential once neutrophils extravasate and travel through the tissue. Our results reveal diminished neutrophil chemotaxis in a 3D matrix in the presence of the NHE1 blocker cariporide and at $pH_e$ 6.5. Therefore, we aimed at elucidating whether this could be due to a reduced amount of activated Cdc42-GTP. Cdc42 activity was determined at two time points following C5a stimulation: after 1 min and after 20 min. Our results reveal that Cdc42 activity in neutrophils is indeed NHE1- and pH-dependent. Notably, Cdc42 activity is much higher at the early time point. However, regardless of the absolute value, there is always an ~60% decrease in the Cdc42-GTP/Cdc42 ratio upon NHE1 inhibition and at $pH_e$ 6.5 (Fig. 9). Interestingly, Cdc42 activity is not inhibited when neutrophils are stimulated with C5a in the presence of cariporide for only 1 min without prior incubation with the NHE1 inhibitor (Supplemental Fig. 4). This observation provides an additional explanation that the observed impairment of neutrophil chemotaxis upon NHE1 inhibition and reduced $pH_e$ both act on Cdc42 activity via an intracellular acidification. We have shown in Fig. 3 that 1 min in $pH_e$ 6.5 or 1 min of NHE1 inhibition is not sufficient to change $pH_i$ significantly.

## Discussion

Tissue acidification affects neutrophil chemotaxis in a distinct way. Chemotaxis has an optimum at a slightly acidic $pH_e$ 7.0, and lowering or increasing the $pH_e$ to 6.8 or 7.4 has little effect. Supporting our observations, chemotactic efficiency in a C5a gradient is augmented when neutrophils are simultaneously exposed to an equally aligned extracellular proton gradient approaching the optimal $pH_e$. Such a $pH_e$ gradient can be encountered by neutrophils in the interstitium after extravasation. Further decreasing $pH_e$ to 6.5 strongly impairs chemotaxis, but neutrophil velocity, a surrogate of the migration motor, is changed to a much lesser extent by variations of the extracellular pH. This suggests that neutrophils chemotax less efficiently once they reach an acidic site of inflammation, but they retain their migratory abilities.

Mechanistically, our results indicate that alterations of $pH_i$ play a decisive role in mediating the effects of an extracellular acidification or NHE1 inhibition. In our view $pH_i$ is a major determinant of the two pH-dependent mechanisms identified in this study: pH-dependent $LTB_4$ release and Cdc42 activity are major causes of the pH dependence of chemotaxis. C5a-stimulated neutrophils release the

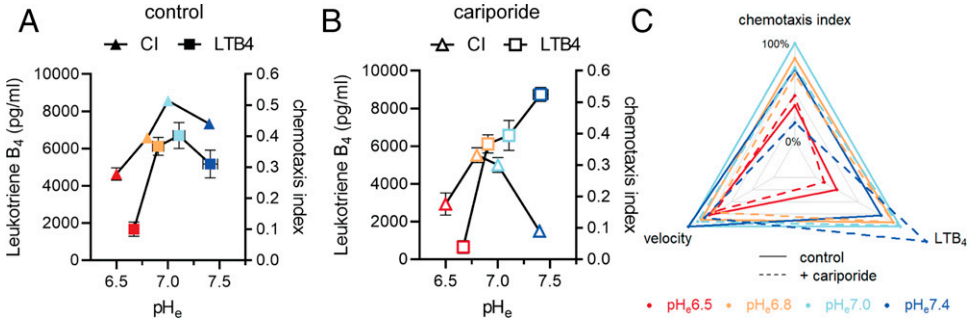


**FIGURE 6.** LTB4 release and chemotaxis indices in different pHe environments. (**A**) Chemotaxis index (CI) and $pH_e$-dependent $LTB_4$ release under control conditions. (**B**) Comparison of $LTB_4$ release and chemotaxis in the presence of the NHE1 inhibitor cariporide. (**C**) Radar chart summarizing migratory abilities (velocity and chemotaxis) with $LTB_4$ production in varied $pH_e$ environments. Values measured at $pH_e$ 7.0 (chemotaxis) and $pH_e$7.1 ($LTB_4$ concentration) are taken as 100%.

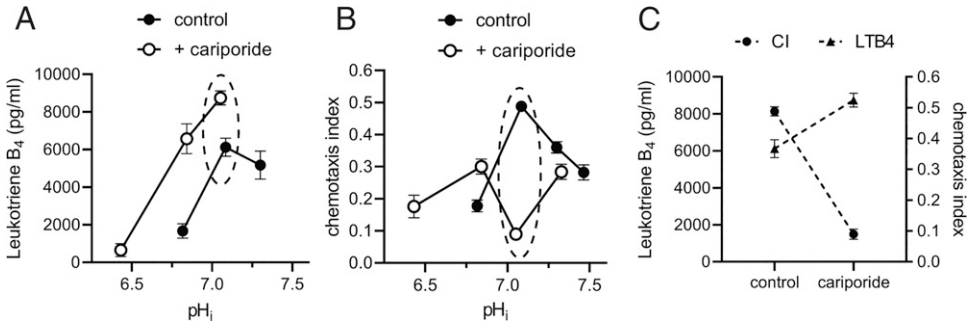


**FIGURE 7.** LTB4 release and chemotaxis as a function of pHi. (**A**) $LTB_4$ production in varied $pH_i$ environments without (closed circles) and with cariporide (open circles). (**B**) Chemotaxis indices in different $pH_i$ environments. (**C**) Comparison of $LTB_4$ production and chemotaxis at $pH_i$ 7.1 (dissected from A and B, circled) without and with cariporide.

maximum amount of $LTB_4$ at $pH_e$ 7.0, and its release is greatly reduced at $pH_e$ 6.5. This apparent $pH_e$ dependence of the $LTB_4$ release mirrors that of chemotaxis. However, during the course of our experiments it became evident that it is rather the *intracellular* than the extracellular pH that affects $LTB_4$ release. Lowering the $pH_i$ by inhibiting NHE1 at an extracellular $pH_e$ 7.4 leads to a seemingly paradoxical increase of the $LTB_4$ release because the intracellular pH shifts to the optimal value for $LTB_4$ release.

So far, it has not yet been studied whether an acidic $pH_e$ or $pH_i$ influences exosomal or intracellular $LTB_4$-producing enzymes. However, an indirect pH-dependent modulation of the $LTB_4$ production is also possible. One of the key enzymes of the $LTB_4$ production cascade, cytosolic phospholipase $A_2$, is stimulated by an increase of the intracellular $Ca^{2+}$ concentration (28). Such an increase of the intracellular $Ca^{2+}$ concentration is induced by C5a, which is at least in part mediated by the activation of Orai1 (29). Orai1, in turn, is inhibited by an extracellular and intracellular acidification (30, 31). Thus, an inhibition of Orai1 by an acidification is expected to lead to a pH-dependent reduction of the $LTB_4$ production.

It is unknown whether the process of exosome secretion by neutrophils is pH-dependent. Interestingly, it was shown that exosome release from carcinoma cells of different tumor entities appears to be regulated in the opposite way. It is increased in an acidic environment (32). We are aware that the nature of cancer cell–derived exosomes may not be the same as those from neutrophils. Nonetheless, the observations made in cancer cells cannot explain our findings of the reduced $LTB_4$ concentration in an acidic supernatant. The observations made in cancer cells would rather argue for an increased production of $LTB_4$ in neutrophils when $pH_e$ is lowered. Undoubtedly, more studies are needed to clarify this question.

Also, the fact that neutrophils may influence the local pericellular pH via exocytosis of acidic vesicles and NHE1 activity can be of importance in the context of neutrophil chemotaxis. Although we did not observe measurable pH changes in the cell matrix upon C5a stimulation, we cannot dismiss the possibility that local pH disturbances may influence other neutrophils migrating in the proximity or modify cell–matrix interactions. We had shown previously that the pericellular $pH_e$ within the glycocalyx regulates migration of melanoma cells NHE1-dependently by controlling $\beta_1$-integrin–mediated cell–matrix adhesion (33, 34). However, such a mechanism is unlikely to account for the observed pH dependence of neutrophil chemotaxis because neutrophil migration in a 3D environment is integrin-independent (20, 35). We therefore propose that the intracellular pH is more important for regulating neutrophil chemotaxis in a 3D environment than the extracellular pH.

A further explanation for the diminished chemotaxis in an acidic pH is given by the fact that $LTB_4$ regulates Cdc42 activation. Cdc42 is a member of the small Rho GTPases family and is crucial for chemotaxis. The role of Cdc42 is underlined by its distribution and asymmetric activation in neutrophil-like PLB-985 cells (18). Hence, the markedly attenuated activation of Cdc42 in an acidic environment is consistent with the impaired chemotaxis efficiency of neutrophils under these conditions. A decrease in $LTB_4$ release in an acidic pH may directly lead to the diminished Cdc42-GTP level. Because $LTB_4$ itself mediates an enhancement of neutrophil chemotaxis (13, 15), it likely triggers the activation of Rho GTPases. Further analysis of Cdc42 activation upon $LTB_4$ stimulation in an acidic pH is required to elucidate this possibility.

The expression of the proton sensing G protein–coupled receptors in neutrophils (e.g., OGR1, TDAG8) (36) may also play a role in the observed response of neutrophils. The activation of TDAG8 by an acidic pH leads to an increased cAMP accumulation in neutrophil-like HL-60 and human neutrophils (37). OGR1 also mediates inositol phosphate formation in several cell lines (38). The involvement of these receptors in pH-dependent neutrophil chemotaxis, however, remains elusive.

Despite high $LTB_4$ production in cells treated with the NHE1 inhibitor at physiological $pH_e$ 7.4 ($pH_i$ 7.05), neutrophil chemotaxis is severely impeded. In this study, we show that NHE1 blockade leads to a reduced activity of Cdc42 in murine neutrophils, as previously shown also in fibroblasts (39) and neurite outgrowth (40).

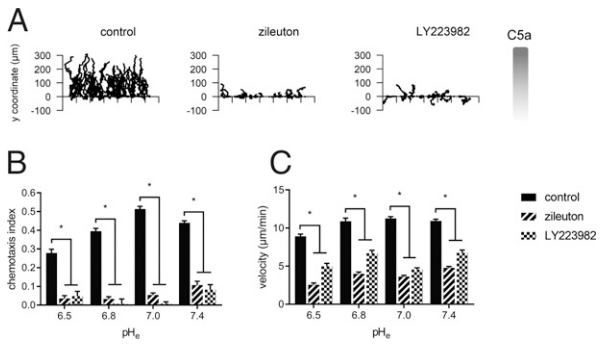


**FIGURE 8.** Neutrophil chemotaxis upon LTB4/BLT1 axis inhibition in different pHe environments. (**A**) Trajectories of individual neutrophils migrating in a 3D collagen I matrix. Trajectories are normalized to common starting points along the *y*-axis, which corresponds to the direction of the C5a gradient. Its direction is indicated on the right-hand side. The left panel shows control experiments at $pH_e$ 7.0. The middle and right panels depict chemotaxis at $pH_e$ 7.0 in the presence of the 5-LOX inhibitor zileuton and the BLT1 blocker LY223982, respectively. (**B**) Mean values of the chemotaxis indices and (**C**) of the velocity at $pH_e$ 6.5–7.4. In (B) and (C) we compare control values with those in the presence of zileuton or LY223982 ($N \geq 3$, $n \geq 60$, Kruskal–Wallis, Dunn's post hoc test). *$p < 0.05$.

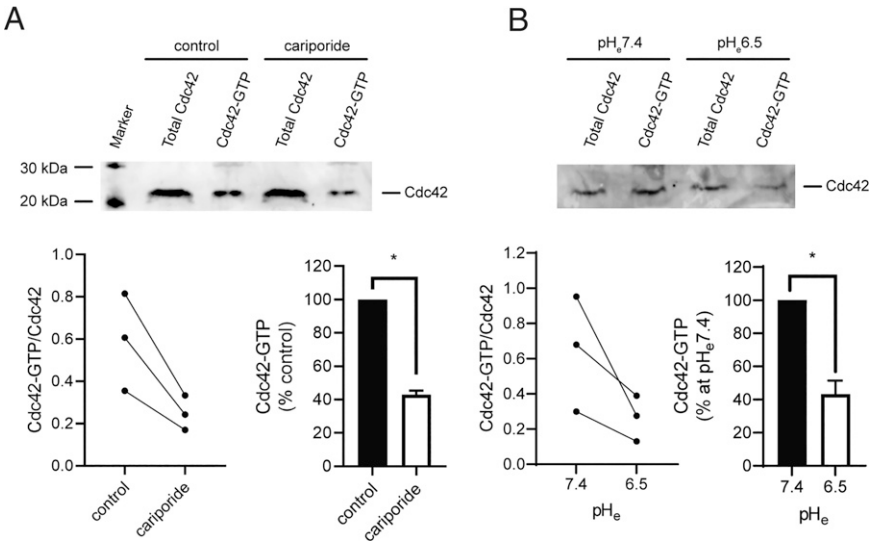


**FIGURE 9.** Cdc42 activation decreases upon NHE1 inhibition and an acidic pHe. (**A**) Pull-down experiments showing the amount of the active Cdc42-GTP form in C5a-stimulated neutrophils without and with cariporide. Neutrophils were pretreated with cariporide (10 μM) for 10 min prior to stimulation with C5a for 1 min. A representative immunoblot (upper panel) of one of the three independent experiments is shown. The lower panel shows a summary of the densitometric evaluation (ratios and normalized data) of the immunoblots ($n$ = 3 replicates of pooled lysates from two mice each). (**B**) Representative immunoblot (upper panel) and densitometric analysis (ratios and normalized data) of neutrophils stimulated with C5a in $pH_e$ 7.4 and 6.5. Neutrophils were pre-equilibrated at $pH_e$ 7.4 or 6.5 for 10 min prior to stimulation with C5a for 1 min ($n$ = 3 replicates of pooled lysates from three mice each).

Thus, it is not surprising that NHE1 inhibition impairs neutrophil chemotaxis as well. According to our findings, NHE1 activity appears to be a prerequisite for chemotaxis toward C5a when $pH_i$ is ~7.1. However, the understanding of the mutual regulation of NHE1, pH, and Rho GTPases such as Rho, Rac, and Cdc42 is far from being complete. There are only few studies showing that Cdc42, Rac1, or RhoA is regulated by the $pH_i$ (39–41). Thus, we cannot rule out that, in addition to Cdc42, the other Rho-GTPases, in particular Rac1, also contribute to pH-dependent neutrophil chemotaxis. RhoA, the major Rho isoform in neutrophils, appears to be an unlikely candidate to account for the inhibition of chemotaxis in an acidic environment. RhoA deletion is accompanied by a hyperactivation of neutrophils (42). Finally, we cannot dismiss the possibility that the effect of pH on small GTPases could be an indirect one: the Ras-specific guanine nucleotide exchange factor RasGRP1 is pH sensitive and would thereby control Ras activity in a pH-dependent manner (43). However, at least in A431 cells, Tiam1, Vav2, and Dock180, which have been implicated in epidermal growth factor receptor–mediated activation of Rac1 and Cdc42, were not affected by changes of $pH_i$ (41).

What is the pathophysiological implication of our findings? The results of our pH-taxis experiments indicate that extravasation of stimulated neutrophils is possibly accelerated by a shallow proton gradient. Along these lines, both pH of the blood and interstitial pH are relevant factors for the recruitment of stimulated neutrophils. Our results also indicate that neutrophil chemotaxis is impaired in the acidic inflammatory microenvironment although the velocity is reduced only to a minor extent. This corroborates results from in vivo studies showing increased neutrophil directionality at the periphery of the injury and rather random motility closer to the insult core (44). We propose that an acidic extracellular pH within an inflammatory focus may contribute to this phenomenon. It is known that neutrophils acquire prolonged survival in an acidic environment and that neutrophil killing mechanisms are reinforced (45). Our observations add to this picture the disrupted neutrophil chemotaxis, which will further contribute to neutrophil retention at the site of inflammation.

## Acknowledgments

We thank Zoltan Pethő for his support and shared expertise in live cell imaging assays. Moreover, we thank Jan Rossaint for the gift of a batch of WEHI-3B cells. We are also grateful to Ilka Neumann for excellent technical assistance.

## Disclosures

The authors have no financial conflicts of interest.

## References

1. Ley, K., H. M. Hoffman, P. Kubes, M. A. Cassatella, A. Zychlinsky, C. C. Hedrick, and S. D. Catz. 2018. Neutrophils: new insights and open questions. *Sci. Immunol.* 3: eaat4579.
2. Leliefeld, P. H. C., C. M. Wessels, L. P. H. Leenen, L. Koenderman, and J. Pillay. 2016. The role of neutrophils in immune dysfunction during severe inflammation. *Crit. Care* 20: 73.
3. Zuo, Y., M. Zuo, S. Yalavarthi, K. Gockman, J. A. Madison, H. Shi, W. Woodard, S. P. Lezak, N. L. Lugogo, J. S. Knight, and Y. Kanthi. 2021. Neutrophil extracellular traps and thrombosis in COVID-19. *J. Thromb. Thrombolysis* 51: 446–453.
4. Erra Díaz, F., E. Dantas, and J. Geffner. 2018. Unravelling the interplay between extracellular acidosis and immune cells. *Mediators Inflamm.* 2018: 1218297.
5. Shi, Y., D. Kim, M. Caldwell, and D. Sun. 2013. The role of $Na^+/H^+$ exchanger isoform 1 in inflammatory responses: maintaining $H^+$ homeostasis of immune cells. *Adv. Exp. Med. Biol.* 961: 411–418.
6. Hayashi, H., O. Aharonovitz, R. T. Alexander, N. Touret, W. Furuya, J. Orlowski, and S. Grinstein. 2008. $Na^+/H^+$ exchange and pH regulation in the control of neutrophil chemokinesis and chemotaxis. *Am. J. Physiol. Cell Physiol.* 294: C526–C534.
7. Morgan, D., M. Capasso, B. Musset, V. V. Cherny, E. Ríos, M. J. S. Dyer, and T. E. DeCoursey. 2009. Voltage-gated proton channels maintain pH in human neutrophils during phagocytosis. *Proc. Natl. Acad. Sci. USA* 106: 18022–18027.
8. Khan, M. A., L. M. Philip, G. Cheung, S. Vadakepeedika, H. Grasemann, N. Sweezey, and N. Palaniyar. 2018. Regulating NETosis: increasing pH promotes NADPH oxidase-dependent NETosis. *Front. Med. (Lausanne)* 5: 19.
9. Panettieri, R. A., Jr. 2018. The role of neutrophils in asthma. *Immunol. Allergy Clin. North Am.* 38: 629–638.
10. O'Neil, L. J., and M. J. Kaplan. 2019. Neutrophils in rheumatoid arthritis: breaking immune tolerance and fueling disease. *Trends Mol. Med.* 25: 215–227.
11. Heit, B., S. Tavener, E. Raharjo, and P. Kubes. 2002. An intracellular signaling hierarchy determines direction of migration in opposing chemotactic gradients. *J. Cell Biol.* 159: 91–102.
12. Petri, B., and M. J. Sanz. 2018. Neutrophil chemotaxis. *Cell Tissue Res.* 371: 425–436.
13. Lämmermann, T., P. V. Afonso, B. R. Angermann, J. M. Wang, W. Kastenmüller, C. A. Parent, and R. N. Germain. 2013. Neutrophil swarms require LTB4 and integrins at sites of cell death in vivo. *Nature* 498: 371–375.
14. Subramanian, B. C., R. Majumdar, and C. A. Parent. 2017. The role of the $LTB_4$-BLT1 axis in chemotactic gradient sensing and directed leukocyte migration. *Semin. Immunol.* 33: 16–29.
15. Subramanian, B. C., K. Moissoglu, and C. A. Parent. 2018. The $LTB_4$-BLT1 axis regulates the polarized trafficking of chemoattractant GPCRs during neutrophil chemotaxis. *J. Cell Sci.* 131: jcs217422.
16. Tackenberg, H., S. Möller, M. D. Filippi, and T. Laskay. 2020. The small GTPase Cdc42 is a major regulator of neutrophil effector functions. *Front. Immunol.* 11: 1197.
17. DeCoursey, T. E. 2016. The intimate and controversial relationship between voltage-gated proton channels and the phagocyte NADPH oxidase. *Immunol. Rev.* 273: 194–218.
18. Yang, H. W., S. R. Collins, and T. Meyer. 2016. Locally excitable Cdc42 signals steer cells during chemotaxis. *Nat. Cell Biol.* 18: 191–201.
19. Sawada, Y., T. Honda, S. Hanakawa, S. Nakamizo, T. Murata, Y. Ueharaguchi-Tanada, S. Ono, W. Amano, S. Nakajima, G. Egawa, et al. 2015. Resolvin E1

inhibits dendritic cell migration in the skin and attenuates contact hypersensitivity responses. *J. Exp. Med.* 212: 1921–1930.
20. Lämmermann, T., B. L. Bader, S. J. Monkley, T. Worbs, R. Wedlich-Söldner, K. Hirsch, M. Keller, R. Förster, D. R. Critchley, R. Fässler, and M. Sixt. 2008. Rapid leukocyte migration by integrin-independent flowing and squeezing. *Nature* 453: 51–55.
21. Lindemann, O., D. Umlauf, S. Frank, S. Schimmelpfennig, J. Bertrand, T. Pap, P. J. Hanley, A. Fabian, A. Dietrich, and A. Schwab. 2013. TRPC6 regulates CXCR2-mediated chemotaxis of murine neutrophils. *J. Immunol.* 190: 5496–5505.
22. Dieterich, P., R. Klages, R. Preuss, and A. Schwab. 2008. Anomalous dynamics of cell migration. *Proc. Natl. Acad. Sci. USA* 105: 459–463.
23. Boron, W. F., and P. De Weer. 1976. Intracellular pH transients in squid giant axons caused by $CO_2$, $NH_3$, and metabolic inhibitors. *J. Gen. Physiol.* 67: 91–112.
24. Klein, M., P. Seeger, B. Schuricht, S. L. Alper, and A. Schwab. 2000. Polarization of $Na^+/H^+$ and $Cl^-/HCO_3^-$ exchangers in migrating renal epithelial cells. *J. Gen. Physiol.* 115: 599–608.
25. Korohoda, W., J. Golda, J. Sroka, A. Wojnarowicz, P. Jochym, and Z. Madeja. 1997. Chemotaxis of *Amoeba proteus* in the developing pH gradient within a pocket-like chamber studied with the computer assisted method. *Cell Motil. Cytoskeleton* 38: 38–53.
26. Sadik, C. D., N. D. Kim, Y. Iwakura, and A. D. Luster. 2012. Neutrophils orchestrate their own recruitment in murine arthritis through C5aR and FcγR signaling. *Proc. Natl. Acad. Sci. USA* 109: E3177–E3185.
27. Majumdar, R., A. Tavakoli Tameh, S. B. Arya, and C. A. Parent. 2021. Exosomes mediate LTB4 release during neutrophil chemotaxis. *PLoS Biol.* 19: e3001271.
28. Clark, J. D., L. L. Lin, R. W. Kriz, C. S. Ramesha, L. A. Sultzman, A. Y. Lin, N. Milona, and J. L. Knopf. 1991. A novel arachidonic acid-selective cytosolic PLA2 contains a $Ca^{2+}$-dependent translocation domain with homology to PKC and GAP. *Cell* 65: 1043–1051.
29. Sogkas, G., T. Vögtle, E. Rau, B. Gewecke, D. Stegner, R. E. Schmidt, B. Nieswandt, and J. E. Gessner. 2015. Orai1 controls C5a-induced neutrophil recruitment in inflammation. *Eur. J. Immunol.* 45: 2143–2153.
30. Scrimgeour, N. R., D. P. Wilson, and G. Y. Rychkov. 2012. $Glu^{106}$ in the Orai1 pore contributes to fast $Ca^{2+}$–dependent inactivation and pH dependence of $Ca^{2+}$ release-activated $Ca^{2+}$ (CRAC) current. *Biochem. J.* 441: 743–753.
31. Gavriliouk, D., N. R. Scrimgeour, S. Grigoryev, L. Ma, F. H. Zhou, G. J. Barritt, and G. Y. Rychkov. 2017. Regulation of Orai1/STIM1 mediated $I_{CRAC}$ by intracellular pH. *Sci. Rep.* 7: 9829.
32. Logozzi, M., E. Spugnini, D. Mizzoni, R. Di Raimo, and S. Fais. 2019. Extracellular acidity and increased exosome release as key phenotypes of malignant tumors. *Cancer Metastasis Rev.* 38: 93–101.
33. Stock, C., B. Gassner, C. R. Hauck, H. Arnold, S. Mally, J. A. Eble, P. Dieterich, and A. Schwab. 2005. Migration of human melanoma cells depends on extracellular pH and $Na^+/H^+$ exchange. *J. Physiol.* 567: 225–238.
34. Ludwig, F. T., A. Schwab, and C. Stock. 2013. The $Na^+/H^+$-exchanger (NHE1) generates pH nanodomains at focal adhesions. *J. Cell. Physiol.* 228: 1351–1358.
35. Reversat, A., F. Gaertner, J. Merrin, J. Stopp, S. Tasciyan, J. Aguilera, I. de Vries, R. Hauschild, M. Hons, M. Piel, et al. 2020. Cellular locomotion using environmental topography. *Nature* 582: 582–585.
36. Okajima, F. 2013. Regulation of inflammation by extracellular acidification and proton-sensing GPCRs. *Cell. Signal.* 25: 2263–2271.
37. Murata, N., C. Mogi, M. Tobo, T. Nakakura, K. Sato, H. Tomura, and F. Okajima. 2009. Inhibition of superoxide anion production by extracellular acidification in neutrophils. *Cell. Immunol.* 259: 21–26.
38. Ludwig, M. G., M. Vanek, D. Guerini, J. A. Gasser, C. E. Jones, U. Junker, H. Hofstetter, R. M. Wolf, and K. Seuwen. 2003. Proton-sensing G-protein-coupled receptors. *Nature* 425: 93–98.
39. Frantz, C., A. Karydis, P. Nalbant, K. M. Hahn, and D. L. Barber. 2007. Positive feedback between Cdc42 activity and $H^+$ efflux by the Na-H exchanger NHE1 for polarity of migrating cells. *J. Cell Biol.* 179: 403–410.
40. Sin, W. C., N. Tam, D. Moniz, C. Lee, and J. Church. 2020. Na/H exchanger NHE1 acts upstream of rho GTPases to promote neurite outgrowth. *J. Cell Commun. Signal.* 14: 325–333.
41. Koivusalo, M., C. Welch, H. Hayashi, C. C. Scott, M. Kim, T. Alexander, N. Touret, K. M. Hahn, and S. Grinstein. 2010. Amiloride inhibits macropinocytosis by lowering submembranous pH and preventing Rac1 and Cdc42 signaling. *J. Cell Biol.* 188: 547–563.
42. Jennings, R. T., M. Strengert, P. Hayes, J. El-Benna, C. Brakebusch, M. Kubica, and U. G. Knaus. 2014. RhoA determines disease progression by controlling neutrophil motility and restricting hyperresponsiveness. *Blood* 123: 3635–3645.
43. Vercoulen, Y., Y. Kondo, J. S. Iwig, A. B. Janssen, K. A. White, M. Amini, D. L. Barber, J. Kuriyan, and J. P. Roose. 2017. A histidine pH sensor regulates activation of the Ras-specific guanine nucleotide exchange factor RasGRP1. *eLife* 6: e29002.
44. Wang, J., M. Hossain, A. Thanabalasuriar, M. Gunzer, C. Meininger, and P. Kubes. 2017. Visualizing the function and fate of neutrophils in sterile injury and repair. *Science* 358: 111–116.
45. Díaz, F. E., E. Dantas, M. Cabrera, C. A. Benítez, M. V. Delpino, G. Duette, J. Rubione, N. Sanjuan, A. S. Trevani, and J. Geffner. 2016. Fever-range hyperthermia improves the anti-apoptotic effect induced by low pH on human neutrophils promoting a proangiogenic profile. *Cell Death Dis.* 7: e2437.